THE IMPORTANCE OF ATMOSPHERIC DIFFERENTIAL REFRACTION IN SPECTROPHOTOMETRY

ALEXEI V. FILIPPENKO

Department of Astronomy, California Institute of Technology, 105-24, Pasadena, California 91125

The effects of atmospheric differential refraction on astronomical measurements are much more important than is generally assumed. In particular, it is shown that relative line and continuum intensities in spectrophotometric work may be erroneous if this phenomenon is neglected. To help observers minimize these errors, the relation between object position and optimal slit or aperture orientation is derived, and practical tables and graphs are presented for use at the telescope.

Key words: instrumentation—observing techniques—spectrophotometry

I. Introduction

Atmospheric differential refraction has long been known to affect the results of a variety of measurement techniques in astronomy. For example, astrometric work requires observations at small zenith angles and comparison of plates taken through similar filter/emulsion combinations—otherwise considerable errors in the derived relative positions of objects may be made (van de Kamp 1967). On the other hand, solar astronomers must often observe through the steady atmosphere shortly after sunrise, and they consequently encounter severe difficulties since different regions of the disk appear along the same line of sight if viewed with a broad-band filter (Simon 1966). Similarly, in spectroscopy a substantial amount of light may be lost at large zenith angles if an object is recorded at a wavelength which differs from the convolution of its energy distribution and the spectral response of the human eye (and/or television guider system).

A related problem at nonzero zenith angles is that more light may be lost from either end of a spectrum than from the center if the object is well-centered in the spectrograph slit at the median wavelengths. This obviously leads to an erroneous measurement of the spectral energy distribution if the wavelength range is large. In view of the recent emphasis placed on relative emission-line intensities in studies of supernovae, planetary nebulae, galactic nuclei, and other objects (e.g., Baldwin, Phillips, and Terlevich 1981), it is important to be aware that even at small air masses the errors may be non-negligible. Although errors can easily be minimized by rotating the spectrograph so that the slit or rectangular aperture is parallel to the direction of atmospheric refraction, a survey of the literature reveals that this practice is generally *not* followed. The purpose of this paper is to remind spectroscopists of the large effects of atmospheric dispersion and to present convenient tables and graphs (for use at the telescope) of optimal slit orientation as a function of object position in the sky.

II. Atmospheric Differential Refraction

A. *Magnitude*

In this section atmospheric differential refraction as a function of wavelength is calculated for the conditions typical of major optical observatories.

At sea level ($P = 760$ mm Hg, $T = 15°$C) the refractive index of dry air is given by (Edlén 1953; Coleman, Bozman, and Meggers 1960)

$$(n(\lambda)_{15,760} - 1)10^6 = 64.328$$
$$+ \frac{29498.1}{146 - (1/\lambda)^2} + \frac{255.4}{41 - (1/\lambda)^2} \, , \tag{1}$$

where λ is the wavelength of light in vacuo (microns). Since observatories are usually located at high altitudes, the index of refraction must be corrected for the lower ambient temperature and pressure (Barrell 1951):

$$(n(\lambda)_{T,P} - 1) = (n(\lambda)_{15,760} - 1)$$
$$\times \frac{P\,[1 + (1.049 - 0.0157\,T)10^{-6}P]}{720.883(1 + 0.003661\,T)} \, . \tag{2}$$

In addition, the presence of water vapor in the atmosphere reduces $(n - 1)10^6$ by

$$\frac{0.0624 - 0.000680/\lambda^2}{1 + 0.003661T}f \, , \tag{3}$$

where f is the water vapor pressure in mm of Hg and T is the air temperature in ° C (Barrell 1951). At an altitude of ~ 2 km and a latitude of $\sim \pm30°$, average conditions are (Allen 1973) $P \approx 600$ mm Hg, $T \approx 7°$ C, and $f \approx 8$ mm Hg. These values are used in equations (1) through (3) in order to obtain $n(\lambda)$, and atmospheric differential refraction (arc seconds) relative to $\lambda = 5000$ Å is then calculated for an object at zenith angle z from (Smart 1931)

$$\Delta R(\lambda) \equiv R(\lambda) - R(5000)$$
$$\approx 206265\,[n(\lambda) - n(5000)]\tan z \, . \tag{4}$$

715

ALEXEI V. FILIPPENKO

The results are presented in Table I. It is clear that the importance of atmospheric dispersion increases rapidly with increasing zenith angle and decreasing wavelength, and infrared observations are rarely affected.

B. *Effect on Spectrophotometry*

Table I demonstrates that at an air mass ($\sim$ sec z) of only 1.1 the image of a point source viewed at 6500 Å is displaced from that at 3500 Å by three-quarters of an arc second, while at sec z = 1.3 the displacement becomes nearly 1.4 arc seconds. It will now be shown that this leads to considerable relative light losses in low- or moderate-dispersion narrow-aperture spectrophotometry if the aperture or slit is *not* aligned along the direction of atmospheric refraction.

The convolution of guiding errors and seeing produces a point spread function whose surface brightness $\mu(r)$ is a Gaussian with dispersion σ (King 1971):

$$\mu(r) = \frac{1}{2\pi\sigma^2} e^{-r^2/2\sigma^2} \quad . \tag{5}$$

This equation is normalized such that the total intensity at any given wavelength is equal to unity, and σ is assumed to be independent of wavelength. If a star is centered at wavelength λ in a rectangular aperture of width $2a$ and length $2b$ (arc seconds), then the amount of light at λ entering the aperture is given by

$$I(\lambda) = \int_{-b}^{b} \int_{-a}^{a} \mu(r)dxdy$$
$$= \frac{1}{2\pi\sigma^2} \int_{-b}^{b} \int_{-a}^{a} e^{-(x^2 + y^2)/2\sigma^2}dxdy \quad , \tag{6}$$

or

$$I(\lambda) = \left(\frac{1}{\sqrt{2\pi}\,\sigma} \int_{-a}^{a} e^{-x^2/2\sigma^2}dx \right)$$
$$\times \left(\frac{1}{\sqrt{2\pi}\,\sigma} \int_{-b}^{b} e^{-y^2/2\sigma^2}dy \right) \quad . \tag{7}$$

On the other hand, if the star is displaced from the aperture center by x_0 arc seconds along the x direction, then

$$I(\lambda) = \frac{1}{2} \left(\frac{1}{\sqrt{2\pi}\,\sigma} \int_{-(a-x_0)}^{(a-x_0)} e^{-x^2/2\sigma^2}dx \right.$$
$$\left. + \frac{1}{\sqrt{2\pi}\,\sigma} \int_{-(a+x_0)}^{(a+x_0)} e^{-x^2/2\sigma^2}dx \right) \tag{8}$$
$$\times \left(\frac{1}{\sqrt{2\pi}\,\sigma} \int_{-b}^{b} e^{-y^2/2\sigma^2}dy \right) \quad .$$

With the aid of standard Gaussian integral tables the above expressions may be easily used to calculate $I(\lambda)$ under various observing conditions.

Suppose, for example, that the spectrum of a star at sec z = 1.1 is obtained with a $2'' \times 4''$ aperture on a night when $2\sigma = 1.''5$, and that the *small* dimension of the aperture is aligned along the atmospheric dispersion. If the star is centered in the aperture at wavelength 5000 Å, then according to Table I it will be off center by $0.''56$ at 3500 Å and by $0.''21$ in the opposite direction at 6500 Å. Consequently, equations (7) and (8) show that the percentage of light entering the aperture at 5000 Å, 6500 Å, and 3500 Å is 81.1, 79.5, and 69.7, respectively. Thus, at an air mass of only 1.1 the light loss at 3500 Å is 11.4 percent greater than at 5000 Å, and it is easy to see that the relative light losses grow rapidly with increasing air mass. These errors are particularly alarming in view of the fact that intensity ratios such as $I([\text{O \sc iii}]\lambda5007)/I([\text{O \sc ii}]\lambda3727)$ are frequently used to distinguish between different ionization mechanisms in galactic nuclei and other objects.

Now suppose that the same conditions apply, except that the *long* dimension of the aperture is oriented along the direction of atmospheric dispersion. Then the percentage of light entering the aperture at 5000 Å, 6500 Å, and 3500 Å is 81.1, 80.9, and 79.5, respectively. The relative light loss has therefore been considerably reduced by proper orientation of the aperture. Furthermore, the losses due to differential refraction disappear entirely if a long slit oriented along the atmospheric refraction is used to obtain widened one-dimensional spectra, since light displaced by different amounts still enters the slit. (Note, however, that problems caused by atmospheric dispersion cannot be completely avoided if unwidened two-dimensional spectra of extended objects are desired.)

III. Optimal Slit or Aperture Position Angle

Since atmospheric differential refraction is perpendicular to the horizon, the slit or rectangular aperture of a spectrograph should be oriented along this direction. When the object is on the meridian, the slit position angle must be 0° or 180°, but as it moves across the sky the angle changes. In this section the optimal slit position angle as a function of object position is derived and tabulated for easy reference. (Following standard practice, the position angle is defined as the angle between the slit and the hour circle through the object, measured from the north through the east from 0° to 360°.)

Consider the spherical triangle whose vertices are defined by the object being observed, the zenith, and the appropriate celestial pole. Application of the law of sines yields

$$\frac{\sin \eta}{\sin (\pi/2 - \phi)} = \frac{\sin h}{\sin z} \quad , \tag{9}$$

where η is the parallactic angle, h is the object's hour angle (h is positive if west of the meridian), z is the object's zenith angle, and ϕ is the observer's latitude. Equa-

Table I

Atmospheric differential refraction at an altitude of 2 km (arcseconds)

Sec z	3000	3500	4000	4500	5000	5500	6000	6500	7000	7500	8000	8500	9000	9500	10000
1.00	0.00	0.00	0.00	0.00	0.00	0.00	0.00	0.00	0.00	0.00	0.00	0.00	0.00	0.00	0.00
1.05	0.68	0.38	0.20	0.08	0.00	-0.06	-0.11	-0.14	-0.17	-0.19	-0.21	-0.23	-0.24	-0.25	-0.26
1.10	0.97	0.55	0.29	0.12	0.00	-0.09	-0.15	-0.20	-0.24	-0.28	-0.30	-0.32	-0.34	-0.36	-0.37
1.15	1.20	0.68	0.36	0.15	0.00	-0.11	-0.19	-0.25	-0.30	-0.34	-0.38	-0.40	-0.42	-0.44	-0.46
1.20	1.40	0.80	0.42	0.17	0.00	-0.13	-0.22	-0.30	-0.35	-0.40	-0.44	-0.47	-0.50	-0.52	-0.54
1.25	1.59	0.90	0.48	0.20	0.00	-0.14	-0.25	-0.33	-0.40	-0.45	-0.50	-0.53	-0.56	-0.59	-0.61
1.30	1.76	1.00	0.53	0.22	0.00	-0.16	-0.28	-0.37	-0.44	-0.50	-0.55	-0.59	-0.62	-0.65	-0.67
1.35	1.92	1.09	0.58	0.24	0.00	-0.17	-0.30	-0.40	-0.48	-0.55	-0.60	-0.64	-0.68	-0.71	-0.73
1.40	2.07	1.18	0.62	0.26	0.00	-0.19	-0.33	-0.44	-0.52	-0.59	-0.65	-0.69	-0.73	-0.77	-0.79
1.45	2.22	1.26	0.67	0.28	0.00	-0.20	-0.35	-0.47	-0.56	-0.63	-0.69	-0.74	-0.79	-0.82	-0.85
1.50	2.37	1.34	0.71	0.29	0.00	-0.21	-0.37	-0.50	-0.60	-0.68	-0.74	-0.79	-0.84	-0.87	-0.91
1.55	2.51	1.42	0.75	0.31	0.00	-0.23	-0.40	-0.53	-0.63	-0.72	-0.78	-0.84	-0.89	-0.93	-0.96
1.60	2.64	1.50	0.80	0.33	0.00	-0.24	-0.42	-0.56	-0.67	-0.75	-0.83	-0.88	-0.93	-0.98	-1.01
1.65	2.78	1.58	0.84	0.34	0.00	-0.25	-0.44	-0.59	-0.70	-0.79	-0.87	-0.93	-0.98	-1.03	-1.06
1.70	2.91	1.65	0.88	0.36	0.00	-0.26	-0.46	-0.61	-0.73	-0.83	-0.91	-0.97	-1.03	-1.07	-1.11
1.75	3.04	1.73	0.92	0.38	0.00	-0.27	-0.48	-0.64	-0.77	-0.87	-0.95	-1.02	-1.07	-1.12	-1.16
1.80	3.17	1.80	0.95	0.39	0.00	-0.29	-0.50	-0.67	-0.80	-0.90	-0.99	-1.06	-1.12	-1.17	-1.21
1.85	3.29	1.87	0.99	0.41	0.00	-0.30	-0.52	-0.69	-0.83	-0.94	-1.03	-1.10	-1.16	-1.22	-1.26
1.90	3.42	1.94	1.03	0.42	0.00	-0.31	-0.54	-0.72	-0.86	-0.98	-1.07	-1.14	-1.21	-1.26	-1.31
1.95	3.54	2.01	1.07	0.44	0.00	-0.32	-0.56	-0.75	-0.89	-1.01	-1.11	-1.19	-1.25	-1.31	-1.36
2.00	3.67	2.08	1.10	0.45	0.00	-0.33	-0.58	-0.77	-0.92	-1.05	-1.15	-1.23	-1.30	-1.35	-1.40
2.10	3.91	2.22	1.18	0.48	0.00	-0.35	-0.62	-0.82	-0.99	-1.12	-1.22	-1.31	-1.38	-1.44	-1.50
2.20	4.15	2.36	1.25	0.51	0.00	-0.37	-0.66	-0.87	-1.05	-1.18	-1.30	-1.39	-1.47	-1.53	-1.59
2.30	4.38	2.49	1.32	0.54	0.00	-0.40	-0.69	-0.92	-1.11	-1.25	-1.37	-1.47	-1.55	-1.62	-1.68
2.40	4.62	2.62	1.39	0.57	0.00	-0.42	-0.73	-0.97	-1.16	-1.32	-1.44	-1.55	-1.63	-1.70	-1.77
2.50	4.85	2.75	1.46	0.60	0.00	-0.44	-0.77	-1.02	-1.22	-1.38	-1.52	-1.62	-1.71	-1.79	-1.86
2.60	5.08	2.88	1.53	0.63	0.00	-0.46	-0.80	-1.07	-1.28	-1.45	-1.59	-1.70	-1.80	-1.88	-1.94
2.70	5.31	3.01	1.60	0.66	0.00	-0.48	-0.84	-1.12	-1.34	-1.51	-1.66	-1.78	-1.88	-1.96	-2.03
2.80	5.54	3.14	1.67	0.69	0.00	-0.50	-0.88	-1.17	-1.40	-1.58	-1.73	-1.85	-1.96	-2.04	-2.12
2.90	5.76	3.27	1.74	0.71	0.00	-0.52	-0.91	-1.21	-1.45	-1.64	-1.80	-1.93	-2.04	-2.13	-2.20
3.00	5.99	3.40	1.80	0.74	0.00	-0.54	-0.95	-1.26	-1.51	-1.71	-1.87	-2.00	-2.12	-2.21	-2.29
3.10	6.21	3.53	1.87	0.77	0.00	-0.56	-0.98	-1.31	-1.57	-1.77	-1.94	-2.08	-2.19	-2.29	-2.38
3.20	6.44	3.65	1.94	0.80	0.00	-0.58	-1.02	-1.36	-1.62	-1.84	-2.01	-2.15	-2.27	-2.38	-2.46
3.30	6.66	3.78	2.00	0.83	0.00	-0.60	-1.05	-1.40	-1.68	-1.90	-2.08	-2.23	-2.35	-2.46	-2.55
3.40	6.88	3.91	2.07	0.85	0.00	-0.62	-1.09	-1.45	-1.73	-1.96	-2.15	-2.30	-2.43	-2.54	-2.63
3.50	7.10	4.03	2.14	0.88	0.00	-0.64	-1.12	-1.50	-1.79	-2.03	-2.22	-2.38	-2.51	-2.62	-2.72
3.60	7.32	4.16	2.20	0.91	0.00	-0.66	-1.16	-1.54	-1.85	-2.09	-2.29	-2.45	-2.59	-2.70	-2.80
3.70	7.54	4.28	2.27	0.94	0.00	-0.68	-1.19	-1.59	-1.90	-2.15	-2.36	-2.52	-2.66	-2.78	-2.88
3.80	7.76	4.41	2.34	0.96	0.00	-0.70	-1.23	-1.64	-1.96	-2.21	-2.42	-2.60	-2.74	-2.86	-2.97
3.90	7.98	4.53	2.40	0.99	0.00	-0.72	-1.26	-1.68	-2.01	-2.28	-2.49	-2.67	-2.82	-2.95	-3.05
4.00	8.20	4.66	2.47	1.02	0.00	-0.74	-1.30	-1.73	-2.07	-2.34	-2.56	-2.74	-2.90	-3.03	-3.14
4.10	8.42	4.78	2.53	1.04	0.00	-0.76	-1.33	-1.77	-2.12	-2.40	-2.63	-2.82	-2.97	-3.11	-3.22
4.20	8.64	4.90	2.60	1.07	0.00	-0.78	-1.37	-1.82	-2.18	-2.46	-2.70	-2.89	-3.05	-3.19	-3.30
4.30	8.85	5.03	2.67	1.10	0.00	-0.80	-1.40	-1.87	-2.23	-2.53	-2.77	-2.96	-3.13	-3.27	-3.39
4.40	9.07	5.15	2.73	1.12	0.00	-0.82	-1.44	-1.91	-2.29	-2.59	-2.83	-3.04	-3.21	-3.35	-3.47
4.50	9.29	5.27	2.80	1.15	0.00	-0.84	-1.47	-1.96	-2.34	-2.65	-2.90	-3.11	-3.28	-3.43	-3.55
4.60	9.51	5.40	2.86	1.18	0.00	-0.86	-1.51	-2.00	-2.40	-2.71	-2.97	-3.18	-3.36	-3.51	-3.64
4.70	9.72	5.52	2.93	1.21	0.00	-0.88	-1.54	-2.05	-2.45	-2.77	-3.04	-3.25	-3.44	-3.59	-3.72
4.80	9.94	5.64	2.99	1.23	0.00	-0.90	-1.57	-2.09	-2.51	-2.84	-3.10	-3.33	-3.51	-3.67	-3.80
4.90	10.15	5.77	3.06	1.26	0.00	-0.92	-1.61	-2.14	-2.56	-2.90	-3.17	-3.40	-3.59	-3.75	-3.88

tion (9) is equivalent to

$$\sin \eta = \frac{\sin h \cos \phi}{[1 - (\sin \phi \sin \delta + \cos \phi \cos \delta \cos h)^2]^{1/2}},$$ (10)

which gives the parallactic angle, and hence the optimal slit position angle, explicitly as a function of object hour angle and declination δ. In practice, one must be very careful when using equation (10) to calculate the slit position angle, as errors are easily made: if we define $-90° \le \eta \le 90°$, then the true position angle may be η, $180° - \eta$, or $-(180° + \eta)$ depending on the hemisphere from which observations are made, on the value of the hour angle, and on whether the object is north or south of the zenith.

In order to minimize relative light losses, it is clearly most desirable to continuously rotate the slit position angle as the object's hour angle changes. Such a system is currently being designed for the 5-m Hale telescope (J. B. Oke 1982). However, for short integrations it is gener-

ally sufficient to use the time-averaged value of the optimal position angle.

Tables II and III list the approximate air mass and best position angle as a function of object hour angle and declination. Air masses are included to aid the observer in deciding whether the differential refraction at the object position (as given in Table I) is of sufficient importance to necessitate rotation of the spectrograph. Although Table II is calculated for the latitude of Palomar Observatory ($\phi = +33°21'$), it is also applicable at many other northern observatories; the only large differences occur when an object is near the zenith, in which case the air mass is so small that differential refraction may be neglected. Similarly, Table III refers specifically to Las Campanas Observatory ($\phi = -29°00'$). Figures 1 and 2 display the optimal position angle versus object hour angle for different object declinations. It is seen that the optimal position angle changes very rapidly for objects near the zenith, but usually the spectrograph need not be rotated in such cases.

Table II

(a) Secant z, and (b) Optimal slit position angle at Palomar Observatory

(a) Hour angle east or west of the meridian

Dec	0.0	0.5	1.0	1.5	2.0	2.5	3.0	3.5	4.0	4.5	5.0	5.5	6.0	6.5	7.0	7.5	8.0
-35.0	2.71	2.75	2.89	3.16	3.61	4.39	5.93	9.88									
-30.0	2.23	2.26	2.36	2.54	2.84	3.34	4.23	6.04									
-25.0	1.91	1.93	2.00	2.14	2.36	2.72	3.30	4.38	6.84								
-20.0	1.68	1.69	1.75	1.86	2.03	2.30	2.72	3.45	4.89	8.90							
-15.0	1.50	1.52	1.57	1.66	1.80	2.01	2.34	2.87	3.83	6.01							
-10.0	1.38	1.39	1.43	1.50	1.62	1.79	2.06	2.47	3.17	4.56	8.51						
-5.0	1.28	1.29	1.32	1.39	1.49	1.63	1.85	2.18	2.72	3.70	5.97						
0.0	1.20	1.21	1.24	1.30	1.38	1.51	1.69	1.97	2.39	3.13	4.63	9.17					
5.0	1.14	1.15	1.17	1.22	1.30	1.41	1.57	1.80	2.16	2.73	3.70	6.39					
10.0	1.09	1.10	1.12	1.17	1.24	1.34	1.48	1.68	1.97	2.44	3.24	4.93					
15.0	1.05	1.06	1.09	1.13	1.19	1.28	1.40	1.58	1.83	2.22	2.85	4.04	7.03				
20.0	1.03	1.03	1.06	1.10	1.15	1.23	1.35	1.50	1.72	2.05	2.56	3.44	5.32				
25.0	1.01	1.02	1.04	1.07	1.13	1.20	1.30	1.44	1.64	1.92	2.33	3.02	4.30	7.49			
30.0	1.00	1.01	1.03	1.06	1.11	1.18	1.27	1.40	1.57	1.81	2.16	2.71	3.64	5.54			
35.0	1.00	1.01	1.02	1.06	1.10	1.17	1.25	1.37	1.52	1.73	2.03	2.47	3.17	4.42	7.23		
40.0	1.01	1.01	1.03	1.06	1.10	1.16	1.24	1.35	1.49	1.67	1.93	2.29	2.83	3.71	5.33	9.22	
45.0	1.02	1.03	1.04	1.07	1.11	1.17	1.24	1.34	1.46	1.63	1.85	2.15	2.57	3.21	4.24	6.15	
50.0	1.04	1.05	1.06	1.09	1.13	1.18	1.25	1.34	1.45	1.60	1.79	2.04	2.37	2.85	3.54	4.64	6.55
55.0	1.08	1.08	1.10	1.12	1.16	1.20	1.27	1.35	1.45	1.58	1.74	1.95	2.22	2.58	3.06	3.75	4.74
60.0	1.12	1.12	1.14	1.16	1.19	1.24	1.30	1.37	1.46	1.57	1.71	1.88	2.10	2.37	2.72	3.16	3.74
65.0	1.17	1.18	1.19	1.21	1.24	1.28	1.34	1.40	1.48	1.58	1.70	1.84	2.01	2.21	2.46	2.75	3.11
70.0	1.25	1.25	1.26	1.28	1.31	1.35	1.39	1.45	1.52	1.60	1.69	1.81	1.94	2.09	2.26	2.46	2.68
75.0	1.34	1.34	1.35	1.37	1.39	1.42	1.46	1.51	1.56	1.63	1.70	1.79	1.88	1.99	2.10	2.23	2.36
80.0	1.46	1.46	1.47	1.48	1.50	1.52	1.55	1.59	1.63	1.68	1.73	1.78	1.85	1.91	1.98	2.06	2.13
85.0	1.61	1.61	1.62	1.63	1.64	1.65	1.67	1.69	1.71	1.74	1.77	1.79	1.83	1.86	1.89	1.92	1.96

(b) Hour angle west of the meridian

Dec	0.0	0.5	1.0	1.5	2.0	2.5	3.0	3.5	4.0	4.5	5.0	5.5	6.0	6.5	7.0	7.5	8.0
-35.0	0.0	6.7	13.3	19.7	25.8	31.5	36.8	41.8									
-30.0	0.0	7.0	13.8	20.3	26.5	32.2	37.4	42.2									
-25.0	0.0	7.3	14.4	21.2	27.5	33.2	38.3	42.9	47.0								
-20.0	0.0	7.8	15.3	22.3	28.7	34.4	39.4	43.8	47.6	51.0							
-15.0	0.0	8.3	16.3	23.6	30.2	35.9	40.8	45.0	48.5	51.5							
-10.0	0.0	9.0	17.6	25.3	32.1	37.8	42.5	46.5	49.7	52.3	54.3						
-5.0	0.0	10.0	19.3	27.5	34.4	40.0	44.6	48.2	51.1	53.3	54.9						
0.0	0.0	11.2	21.5	30.2	37.2	42.8	47.1	50.3	52.8	54.5	55.7	56.4					
5.0	0.0	12.9	24.4	33.6	40.8	46.1	50.0	52.8	54.8	56.0	56.8	57.0					
10.0	0.0	15.3	28.3	38.1	45.1	50.0	53.4	55.6	57.1	57.8	58.0	57.8					
15.0	0.0	19.0	33.9	44.0	50.5	54.7	57.4	58.9	59.7	59.8	58.7	57.6					
20.0	0.0	25.0	41.9	51.7	57.2	60.3	62.0	62.7	62.7	62.2	61.3	59.9	58.3				
25.0	0.0	36.3	54.0	61.7	65.3	66.8	67.2	66.9	66.0	64.8	63.2	61.4	59.2	56.7			
30.0	0.0	60.4	71.4	74.2	74.7	74.1	73.0	71.5	69.7	67.7	65.5	63.0	60.3	57.4			
35.0	180.0	102.8	93.3	88.6	85.2	82.1	79.3	76.5	73.8	70.9	68.0	64.9	61.7	58.2	54.6		
40.0	180.0	135.6	114.3	103.2	96.0	90.5	86.0	81.9	78.1	74.4	70.7	67.0	63.2	59.3	55.2	50.9	
45.0	180.0	151.0	130.1	116.2	106.4	98.9	92.8	87.5	82.6	78.1	73.7	69.4	65.0	60.6	56.1	51.5	
50.0	180.0	158.8	140.8	126.6	115.7	106.9	99.5	93.1	87.4	82.0	76.9	72.0	67.1	62.2	57.3	52.2	47.1
55.0	180.0	163.3	148.0	134.7	123.6	114.1	105.9	98.7	92.1	86.0	80.3	74.7	69.3	64.0	58.6	53.2	47.7
60.0	180.0	166.2	153.0	140.9	130.1	120.5	111.8	104.0	96.8	90.1	83.8	77.7	71.8	66.0	60.2	54.4	48.7
65.0	180.0	168.1	156.6	145.6	135.4	125.9	117.2	109.0	101.4	94.3	87.4	80.8	74.5	68.2	62.0	55.9	49.8
70.0	180.0	169.5	159.2	149.2	139.7	130.5	121.9	113.6	105.8	98.3	91.1	84.1	77.3	70.7	64.1	57.7	51.3
75.0	180.0	170.6	161.3	152.1	143.1	134.4	125.9	117.8	109.8	102.2	94.7	87.4	80.3	73.4	66.5	59.7	53.0
80.0	180.0	171.4	162.8	154.3	145.9	137.6	129.5	121.5	113.6	105.9	98.3	90.8	83.5	76.2	69.1	62.0	55.0
85.0	180.0	172.0	164.0	156.1	148.2	140.3	132.5	124.7	117.0	109.3	101.7	94.2	86.7	79.3	71.9	64.6	57.3

Note: The corresponding position angles for objects east of the meridian are negative.

Many spectrographs capable of being rotated are set by default to a position angle of 90°. Although this minimizes light losses caused by tracking errors, the losses due to atmospheric dispersion may be far larger. Since objects are frequently observed when they are near the meridian, the optimal position angle is often closer to 0° or 180° rather than to the default value. Thus, erroneous relative line strengths pervade the literature and must be viewed with caution. Only the best available data should be incorporated in astrophysical models, as was generally done by Baldwin et al. (1981).

REFERENCES

Allen, C. W. 1973, Astrophysical Quantities, 3rd ed. (London: Athlone Press), pp. 119–22.

Baldwin, J. A., Phillips, M. M., and Terlevich, R. 1981, Pub. A.S.P. 93, 5.

Barrell, H. 1951, J. Opt. Soc. Am. 41, 295.

Coleman, C. D., Bozman, W. R., and Meggers, W. F. 1960, Tables of Wavenumbers, N.B.S. Monograph 3, Washington, p. IV.

Edlén, B. 1953, J. Opt. Soc. Am. 43, 339.

King, I. R. 1971, Pub. A.S.P. 83, 199.

Oke, J. B. 1982 (private communication).

Simon, G. W. 1966, A.J. 71, 190.

Smart, W. M. 1931, Textbook on Spherical Astronomy, 6th ed. (1977) (Cambridge: Cambridge University Press), p. 61.

van de Kamp, P. 1967, Principles of Astrometry (San Francisco: W. H. Freeman and Co.), chap. 6.

Table III

(a) Secant z, and (b) Optimal slit position angle at Las Campanas Observatory

(a) Hour angle east or west of the meridian

Dec	0.0	0.5	1.0	1.5	2.0	2.5	3.0	3.5	4.0	4.5	5.0	5.5	6.0	6.5	7.0	7.5	8.0
35.0	2.28	2.31	2.42	2.61	2.92	3.44	4.38	6.33									
30.0	1.94	1.97	2.04	2.19	2.42	2.79	3.41	4.57	7.34								
25.0	1.70	1.72	1.78	1.90	2.08	2.36	2.81	3.60	5.22								
20.0	1.52	1.54	1.59	1.68	1.83	2.06	2.41	2.99	4.08	6.72							
15.0	1.39	1.40	1.45	1.53	1.65	1.84	2.12	2.57	3.37	5.06							
10.0	1.29	1.30	1.34	1.41	1.51	1.67	1.91	2.27	2.89	4.07	7.21						
5.0	1.21	1.22	1.25	1.31	1.40	1.54	1.74	2.05	2.54	3.43	5.46						
0.0	1.14	1.15	1.18	1.24	1.32	1.44	1.62	1.88	2.29	2.99	4.42	8.76					
-5.0	1.09	1.10	1.13	1.18	1.25	1.36	1.52	1.75	2.09	2.66	3.73	6.41					
-10.0	1.06	1.07	1.09	1.14	1.20	1.30	1.44	1.64	1.94	2.42	3.26	5.09					
-15.0	1.03	1.04	1.06	1.10	1.17	1.26	1.38	1.56	1.83	2.23	2.91	4.24	7.97				
-20.0	1.01	1.02	1.04	1.08	1.14	1.22	1.34	1.50	1.73	2.08	2.64	3.66	6.03				
-25.0	1.00	1.01	1.03	1.07	1.12	1.20	1.31	1.45	1.66	1.97	2.44	3.24	4.88	9.86			
-30.0	1.00	1.01	1.03	1.06	1.11	1.19	1.29	1.42	1.61	1.88	2.28	2.93	4.13	6.97			
-35.0	1.01	1.01	1.03	1.06	1.11	1.18	1.27	1.40	1.57	1.81	2.16	2.69	3.60	5.42			
-40.0	1.02	1.02	1.04	1.07	1.12	1.19	1.27	1.39	1.55	1.76	2.06	2.51	3.21	4.46	7.23		
-45.0	1.04	1.05	1.06	1.09	1.14	1.20	1.28	1.39	1.53	1.73	1.99	2.36	2.92	3.82	5.47	9.42	
-50.0	1.07	1.08	1.09	1.12	1.17	1.22	1.30	1.40	1.53	1.70	1.93	2.25	2.69	3.36	4.43	6.40	
-55.0	1.11	1.12	1.13	1.16	1.20	1.26	1.33	1.42	1.54	1.70	1.90	2.16	2.52	3.02	3.74	4.87	6.84
-60.0	1.17	1.17	1.19	1.21	1.25	1.30	1.37	1.46	1.57	1.70	1.88	2.10	2.38	2.76	3.26	3.96	4.97
-65.0	1.24	1.24	1.26	1.28	1.32	1.36	1.43	1.51	1.60	1.72	1.87	2.05	2.28	2.56	2.91	3.36	3.93
-70.0	1.33	1.33	1.34	1.37	1.40	1.44	1.50	1.57	1.65	1.75	1.88	2.02	2.20	2.40	2.64	2.93	3.27
-75.0	1.44	1.44	1.46	1.48	1.51	1.54	1.59	1.65	1.72	1.80	1.90	2.01	2.14	2.28	2.44	2.62	2.82
-80.0	1.59	1.59	1.60	1.62	1.64	1.67	1.71	1.75	1.81	1.87	1.94	2.01	2.09	2.19	2.28	2.38	2.49
-85.0	1.79	1.79	1.80	1.81	1.82	1.84	1.86	1.89	1.92	1.95	1.99	2.03	2.07	2.11	2.16	2.20	2.25

(b) Hour angle west of the meridian

Dec	0.0	0.5	1.0	1.5	2.0	2.5	3.0	3.5	4.0	4.5	5.0	5.5	6.0	6.5	7.0	7.5	8.0
35.0	180.0	172.7	165.6	158.7	152.3	146.2	140.6	135.4									
30.0	180.0	172.4	165.0	157.9	151.3	145.2	139.7	134.7	130.1								
25.0	180.0	171.9	164.1	156.8	150.1	144.0	138.6	133.8	129.5								
20.0	180.0	171.4	163.1	155.4	148.5	142.5	137.2	132.6	128.6	125.2							
15.0	180.0	170.6	161.8	153.7	146.6	140.6	135.5	131.1	127.5	124.5							
10.0	180.0	169.7	160.1	151.6	144.3	138.3	133.4	129.2	125.3	123.5	121.5						
5.0	180.0	168.4	157.9	148.8	141.5	135.6	131.0	127.3	124.5	122.4	120.8						
0.0	180.0	166.7	155.0	145.4	137.9	132.3	128.1	124.9	122.6	121.0	119.8	119.2					
-5.0	180.0	164.3	151.1	140.9	133.6	128.4	124.8	122.2	120.4	119.3	118.7	118.6					
-10.0	180.0	160.7	145.6	135.2	128.3	123.8	120.9	119.0	117.9	117.4	117.4	117.8					
-15.0	180.0	154.9	137.8	127.7	121.9	118.5	116.5	115.5	115.1	115.3	115.9	116.8	118.2				
-20.0	180.0	144.3	126.4	118.2	114.2	112.3	111.5	111.5	112.0	112.9	114.1	115.7	117.5				
-25.0	180.0	122.6	110.0	106.3	105.3	105.3	106.1	107.2	108.6	110.2	112.1	114.3	116.7	119.4			
-30.0	0.0	83.2	89.4	92.7	95.4	97.8	100.1	102.5	104.9	107.4	110.0	112.7	115.6	118.8			
-35.0	0.0	48.7	68.9	78.8	85.1	89.9	93.9	97.5	100.9	104.2	107.6	110.9	114.4	118.1			
-40.0	0.0	31.5	52.8	66.1	75.2	82.0	87.6	92.4	96.8	100.9	105.0	109.0	113.0	117.2	121.5		
-45.0	0.0	22.9	41.6	55.7	66.2	74.5	81.3	87.2	92.5	97.5	102.2	106.8	111.4	116.0	120.8	125.6	
-50.0	0.0	17.9	34.0	47.4	58.4	67.6	75.3	82.1	88.2	93.9	99.3	104.5	109.6	114.7	119.9	125.1	
-55.0	0.0	14.8	28.7	41.1	51.9	61.4	69.7	77.2	84.0	90.3	96.3	102.0	107.6	113.2	118.8	124.4	130.0
-60.0	0.0	12.7	24.8	36.2	46.6	56.0	64.6	72.5	79.8	86.6	93.1	99.4	105.5	111.5	117.4	123.4	129.4
-65.0	0.0	11.1	22.0	32.4	42.2	51.5	60.1	68.2	75.8	83.1	90.0	96.7	103.2	109.6	115.9	122.2	128.4
-70.0	0.0	10.0	19.8	29.4	38.7	47.6	56.1	64.3	72.1	79.6	86.8	93.9	100.7	107.5	114.1	120.7	127.3
-75.0	0.0	9.1	18.1	27.1	35.8	44.3	52.7	60.7	68.6	76.2	83.7	91.0	98.2	105.2	112.2	119.0	125.9
-80.0	0.0	8.4	16.8	25.2	33.5	41.6	49.7	57.6	65.4	73.1	80.7	88.1	95.5	102.8	110.0	117.1	124.2
-85.0	0.0	7.9	15.8	23.7	31.5	39.4	47.1	54.9	62.6	70.2	77.8	85.3	92.8	100.2	107.6	114.9	122.2

Note: The corresponding position angles for objects east of the meridian are negative.
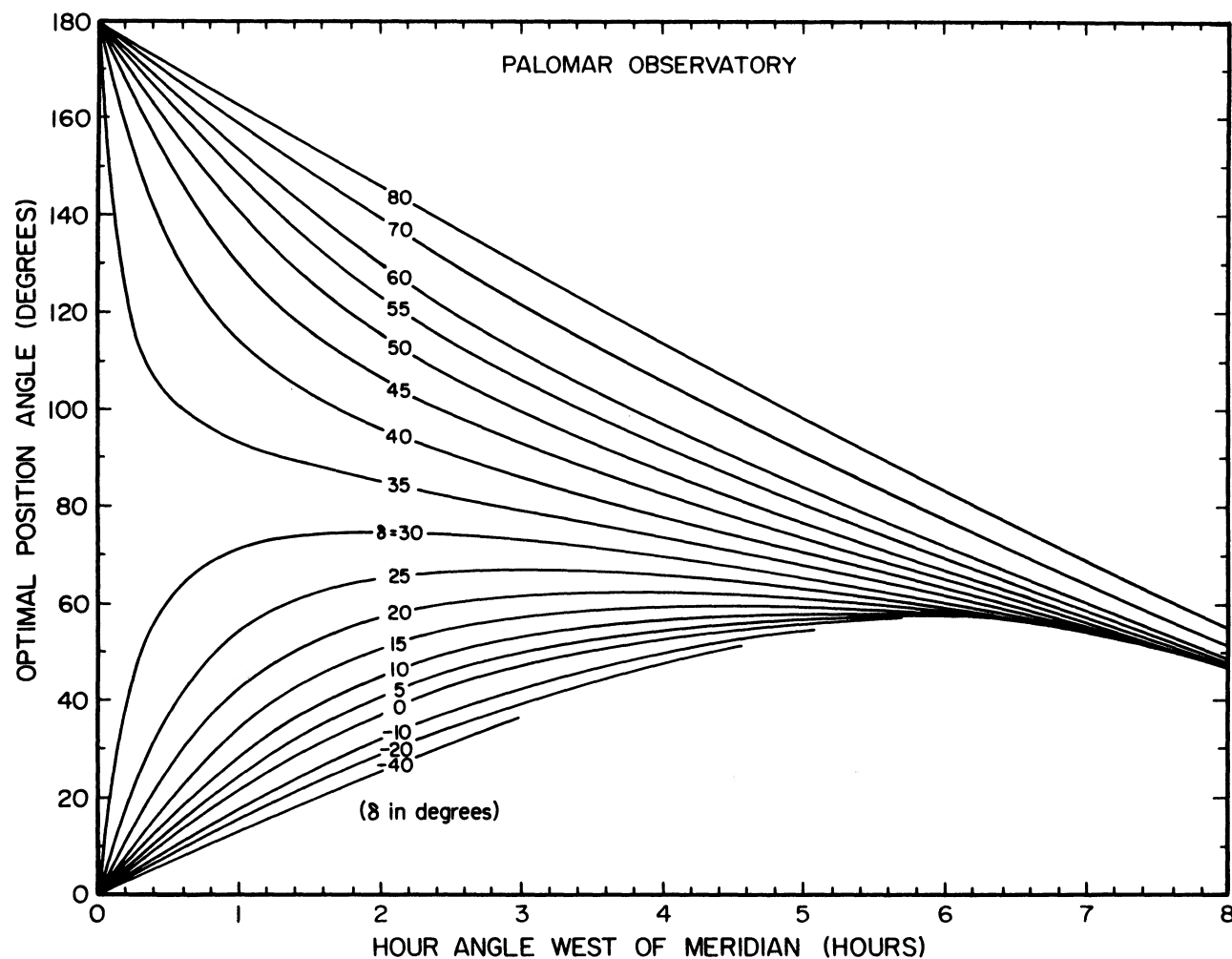
FIG. 1—Optimal slit or aperture position angle as a function of object position west of the meridian, computed for the latitude of Palomar Observatory. The diagram is valid for most other major observatories in the Northern Hemisphere, except at very small air masses. Corresponding position angles for objects east of the meridian are negative.
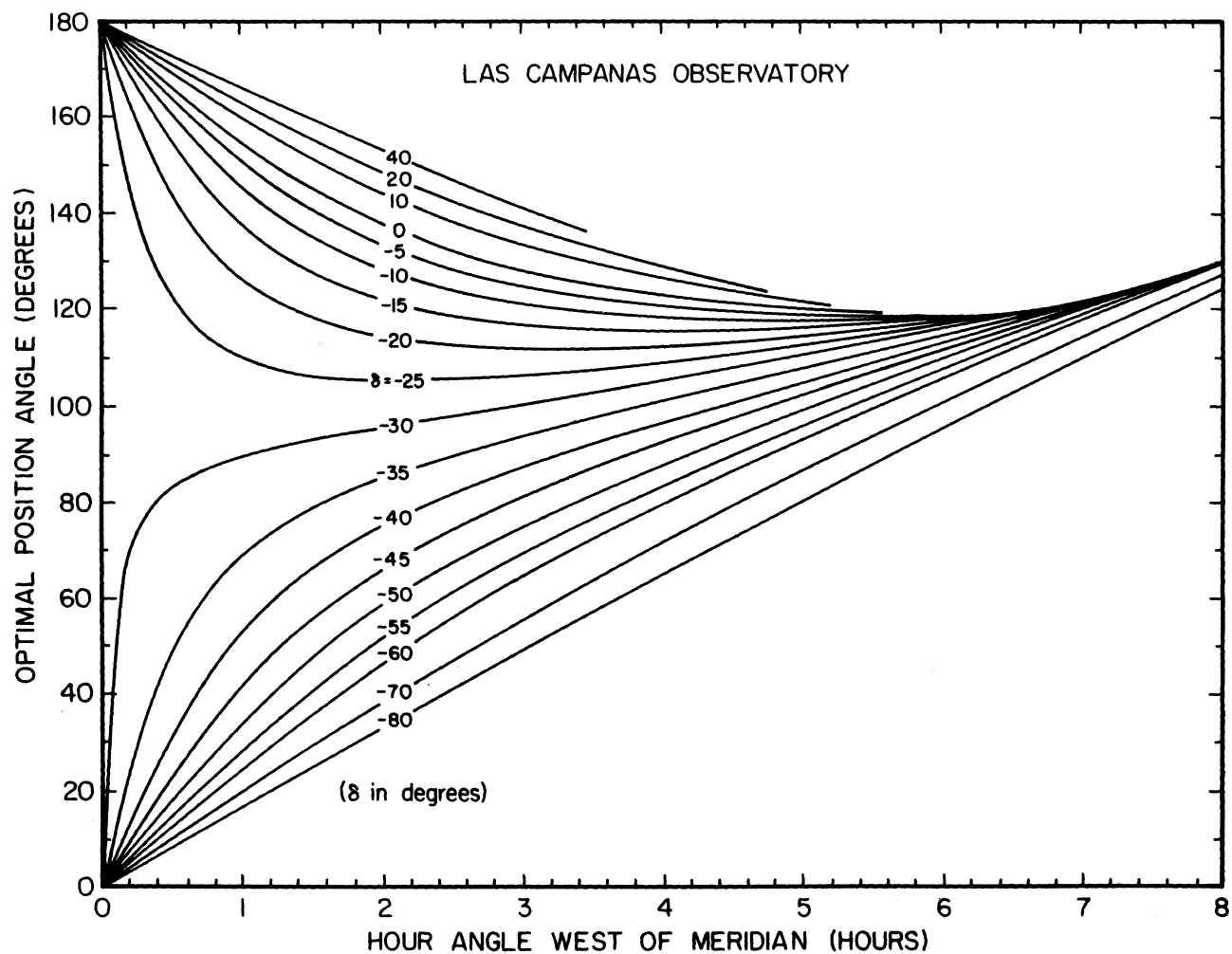
FIG. 2—The same as Figure 1, but computed for the latitude of Las Campanas Observatory. The diagram is valid for most other major observatories in the Southern Hemisphere, except at very small air masses.